Bachelor's Thesis

Radboud University
Department of High Energy Physics

Sterile Neutrinos as Dark Matter

Exploring a 3+3 Type-I Seesaw Model and the Possibility of Sterile Neutrino Dark Matter

Author:
Bart Steeman

Supervisors:
Prof. dr. W.J.P. Beenakker &
J.W. Kip MSc

Second Reader:
Dr. C.F. Galea

April 14, 2021

Contents

1. Introduction

One of the big open questions in physics is the exact nature of dark matter (DM), which comprises the lion's share of the matter content in the universe. Unlike normal matter we can not observe DM with traditional methods. Many possible DM candidates have been put forward. They range from objects like black holes and neutron stars, massive but radiating too faintly for us to observe, to theorized elementary particles like neutralinos and axions. This thesis is concerned with another theorized particle, but one with a more familiar name: the neutrino. However we have to be careful not to confuse it with the three flavours of neutrinos[1] we know from the Standard Model (SM). Our candidate is the sterile neutrino.

The SM describes the known elementary particles and their properties. It is a powerful tool, but it has some flaws. First of all, in the original formulation of the SM neutrinos do not have mass. But now it is known that neutrinos are able to oscillate between the three flavour states. For example, electron neutrinos produced in the sun may have switched to muon neutrinos by the time they arrive on earth. This is only possible if there is a mass difference between the mass eigenstates of the neutrinos, so the neutrinos can not all be massless. Secondly, none of the particles described in the SM are possible DM candidates. They are either charged (and thus detectable) or, in the case of the neutrinos, they are too light[1].

So the question arises if we can find a way to solve both of our problems with one theoretical model. There are models that expand or in other ways modify the SM. An example of that would be the minimal supersymmetric model, which can provide a DM candidate in the form of the lightest neutralino[2], but does not have a solution for our neutrino mass problem. Our hope lies with the sterile neutrinos. They are heavy, right-handed neutrinos that do not interact with any of the SM forces. The model discussed in this thesis adds three of these to the SM. We will explain how they can generate mass for our 'normal' active neutrinos through the type-I seesaw mechanism and what necessary conditions there are for a sterile neutrino to be a proper DM candidate. We will also perform a search through the model's parameter space to see if we can produce points that satisfy both the known mass differences of the SM neutrinos and the experimental constraints for DM.

In the first three chapters of this thesis we will lay out the necessary theoretical background to understand the type-I seesaw mechanism and the relevance of sterile neutrinos in the context of DM. Chapter 2 serves as an introduction to DM, chapter 3

[1] The electron neutrino, muon neutrino and tau neutrino.

[2] Or the lightest sneutrino, a supersymmetric partner of the neutrinos.

discusses the SM and the physics of neutrino oscillations, and chapter 4 introduces the type-I seesaw mechanism. In chapter 5 we explore our chosen model. We explain the methods used to acquire data and our choice of parameters, and show the important results. In chapter 6 we look at our data in the context of DM. We look at the experimental constraints on sterile neutrino DM and compare it to our results. We also shortly discuss the νMSM (Neutrino Minimal SM). In addition to neutrino masses and DM, this model tries to explain the asymmetry between the matter and antimatter content of our universe with the addition of three sterile neutrinos.

2. Dark Matter

We do not yet know the nature of DM, but we have a better idea of how much of it there is in the universe. Only 5% of the matter-energy content of the universe consists of the ordinary matter we know and see around us. The rest is made up of so called dark energy (69%) and DM (26%) [2]. So in total 84% of all matter is DM. 'Dark' in this context means that we are not able to observe it with telescopes in any part of the electromagnetic spectrum. This either implies that it does not emit electromagnetic radiation with enough intensity to be picked up by telescopes, or that it has no electromagnetic or strong interactions at all.

This makes it difficult to detect DM, and it begs the question why we believe in the existence of DM in the first place. This is not because it was directly detected, but because of the observation of several gravitational effects that imply the presence of large amounts of additional mass (in addition to observable objects like stars and gas) in certain regions of space.

2.1 Rotations, Lensing and Bullets

One of the first hints towards the existence of DM came from studying the orbital rotation of stars in galaxies [3]. It turns out that the observed luminous matter in a galaxy cannot explain the observed orbital velocities of its stars. From Kepler's laws you expect the rotational velocity within a galaxy to decrease with roughly $\frac{1}{\sqrt{r}}$ after a certain distance from the galactic center. However, as we see in Fig. 2.1 the observed rotation curve of galaxy NGC 6503 first rises and then flattens off to a constant velocity. This type of curve has been repeatedly observed in other galaxies.

DM was proposed as a model to explain this discrepancy between the observed and expected rotation curves. In addition to the visible stellar mass and gas disk, a halo of non-luminous matter is added to the galaxy. If it is given the right density profile (where this DM halo typically contributes most of the total mass of the galaxy) the observed rotation curve can be reproduced.

More evidence was found through gravitational lensing. The theory of general relativity states that space is curved in the presence of (large amounts of) mass. Light that passes through curved space appears to travel along a curved line from an outside perspective. If there is a large concentration of mass, for example in the form of a cluster of galaxies, the curvature of space in its vicinity acts in a similar way as an optical lens. If such a lens is present between us as observers and a bright celestial object, the light from this object will pass the gravitational lens, bending

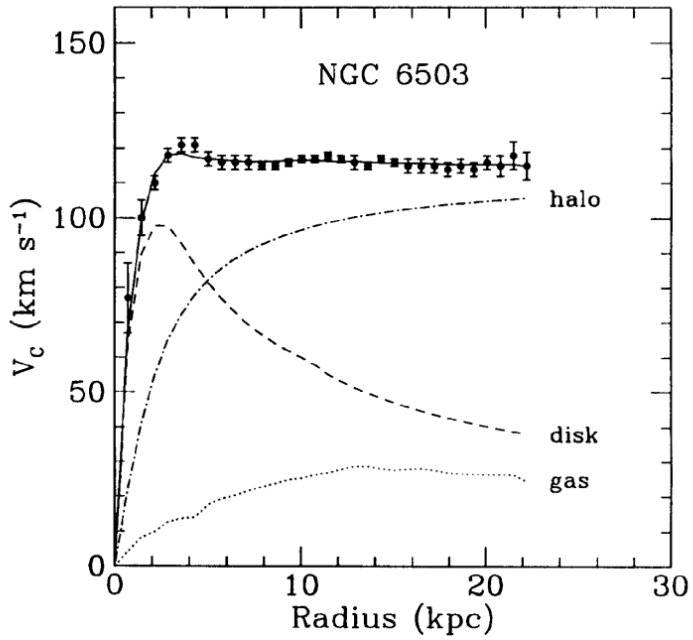

Figure 2.1: Rotation curve for the NGC 6503 galaxy. The solid line represents the fitted line to the observed data. The dotted and dashed lines give the calculated contributions of the luminous matter for respectively the gas and the stellar disk. The halo represents the DM contribution necessary to match the observed curve [3]

and distorting it before it arrives at the observer. So, if there is DM present in the lens galaxy cluster we expect to see a larger amount of bending and distortion than predicted based on only the observable mass content. Observations from the Hubble Space Telescope (Fig. 2.2) have confirmed that this is exactly what happens. Additionally, we see that DM is not only present within galaxies, but it extends outside of them as well.

An interesting result is found when we use gravitiational lensing to study the Bullet Cluster. It was formed from the collision of two smaller clusters of galaxies. Fig. 2.3 shows the current distribution of baryonic matter (pink) and DM (violet). During the collision the baryonic gas of the two systems experienced friction (from fundamental particle interactions) and settled relatively close to the center of the collision. But both the stellar (stars only interact gravitationally with each other during the collision) and DM content of the galaxies experienced less friction and only settle after travelling some distance. This indicates that DM does not interact as strongly as baryonic matter, presumably because it does not couple to all fundamental forces, or at least that its couplings are not as strong.

2.2 CMB and Relic Density

More evidence for the existence of DM comes from the Cosmic Microwave Background (CMB). The CMB is is a faint radiation present everywhere in our universe that is predicted by Big Bang models. It is the earliest emitted radiation and stems

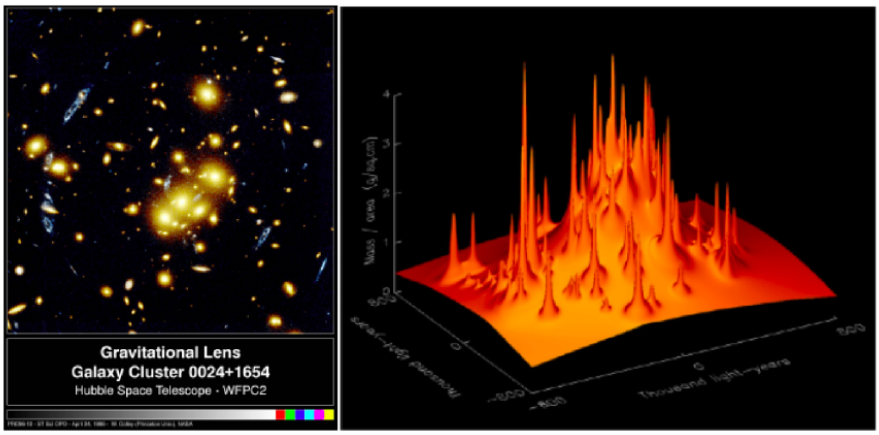

Figure 2.2: Left: Gravitational lensing. The galaxy cluster in the foreground (yellow) acts as a gravitational lens on the light from a galaxy in the background (blue), resulting in multiple distorted images of the background galaxy. Right: A reconstruction of the mass density of the galxay cluster in the foreground. The peaks represent the location of galaxies in the cluster. There is a smooth non-zero background of matter present that also extends outside of the stellar content of the galaxy. [3]

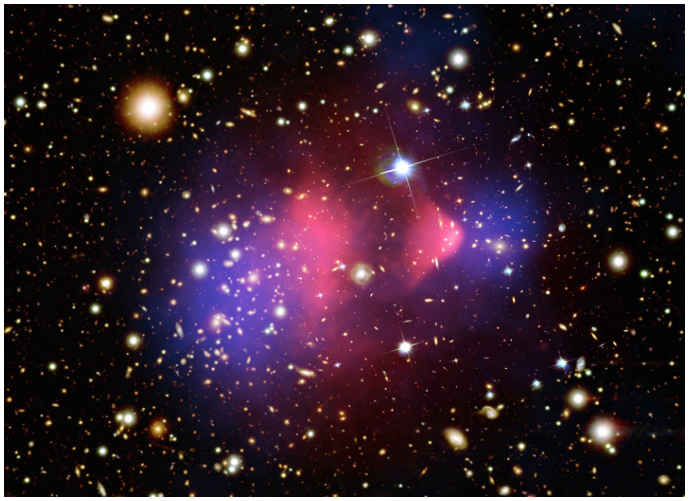

Figure 2.3: The distribution of 'normal' baryonic mass (pink) and DM (violet) present in the Bullet Cluster after collision [4].

from early in the formation of the universe, at the point that it cooled down enough that electrons got bound to nuclei. That allowed photons to move without almost immediately interacting with free electrons. It was first accidentally measured in the 1940's, and measurements have continued to improve over the years. This is important because the CMB is slightly anisotropic, meaning that the temperature of the signal is not the same from every direction on the sky (See Fig. 2.4). These measurements of the first radiation provide us with information about the formation and the early moments of the universe. Most importantly for us the measurements of the CMB agree with the existence of DM, and they give us a number for the current DM relic density. We know from measurements of the CMB that the DM relic density is $\Omega h^2 = 0.1200 \pm 0.0012$.[2][1]

[1]These results are based on the λCDM model and uses its standard assumptions.

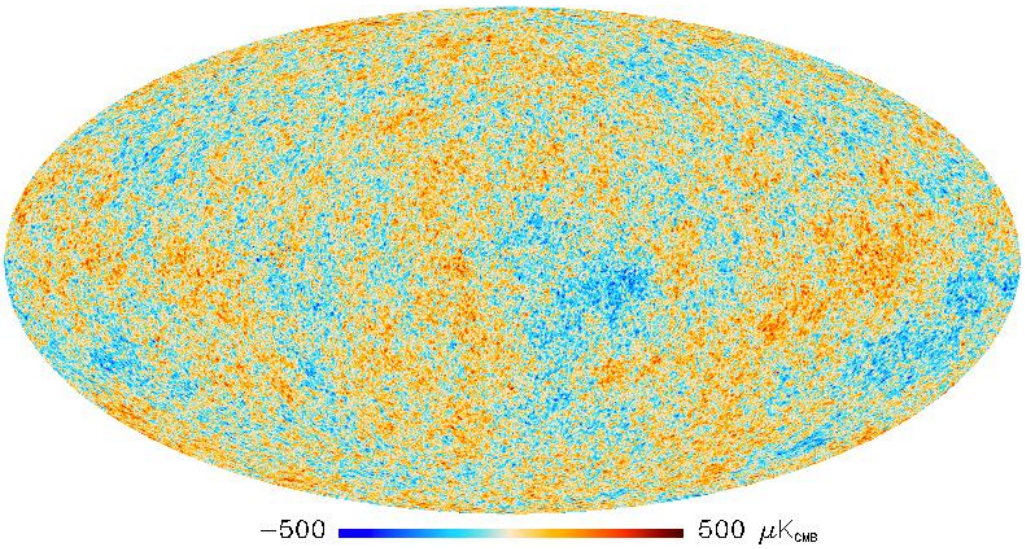

Figure 2.4: Sky map of the Cosmic Microwave Background measured by the Planck Observatory.[5]

The relic density is a quantity that tells us how much of the DM that was produced in the early universe is still around at present (assuming that DM consists of particles). The early universe was hot, and particles existed in a thermal equilibrium where they were produced and annihilated through different interactions at high rates. But as the universe expanded its temperature dropped. At a certain temperature the particle decouples from the rest of the cosmic soup. Its production and annihilation processes slow down significantly, so much that its total amount will barely change for the rest of the lifespan of the universe (or at least up to present day). This process is known as the freeze-out. The amount of DM at its freeze-out and the expansion of the universe determine the current DM relic density.

If we have a theoretical model with a DM particle candidate we want to know for what range of masses and (annihilation) cross-sections it reproduces the correct DM relic density. We can do this by solving the Boltzmann equation [4], while taking into account all creation and annihilation processes of this particle.[2]

$$\dot{n}(t) + 3H(t)n(t) = -\langle\sigma v\rangle(n(t)^2 - n_{eq}(t)^2) \tag{2.1}$$

Here $n(t)$ is the DM particle density as a function of time and n_{eq} is the particle density during equilibrium. H is the Hubble constant that accounts for the expansion of the universe. The right-hand term describes DM production and annihilation, where $\langle\sigma v\rangle$ is the thermally averaged velocity weighted total cross section.

Additionally we can say that a DM particle must be a stable particle, or have a half life longer than the age of the universe. If it were shorter the amount of DM particles would have decreased significantly since freeze-out by decaying, and the current DM relic density would be much lower.

[2]Because of the large number of processes involved these calculations become quite complex, and are generally done numerically.

2.3 MACHO, WIMP or Something Else

The list of proposed DM candidates is long, but we will quickly discuss a few and their viability. It is important to note that DM is not necessarily made up of only one type of particle or type of object, and several candidates together could contribute to the total amount of DM observed, but most research is focused on finding a single candidate that can at least explain the majority of the DM relic density.

- **MACHOs** (MAssive Compact Halo Objects) is an umbrella term for massive objects that are made up of baryonic matter, but are too faint to observe with current telescope resolutions. Examples include faint stars or stellar remains (neutron stars, white dwarfs) and black holes. Observations that look at gravitational lensing effects from faint objects like planets and MACHOs (microlensing) have largely excluded that MACHOs contribute significantly to the total DM content. It is still possible that they contribute to the DM mass content of galaxies to some degree. For example, white dwarfs possibly contribute up to 15% of the DM content in the Milky Way [3].

- **WIMPs** (Weakly Interacting Massive Particles) are massive particles that do not participate in electromagnetic or strong interactions, and are only subject to interactions at the order of strength of the weak force. They are a popular class of DM candidates, mainly because of something known as the WIMP miracle. If their mass is in the range of 1 GeV to 10 TeV they reproduce the correct DM relic density because of their (lack of) interactions.[3] The biggest problem for WIMPs is that they have yet to be detected in collider experiments, which puts increasingly more stringent limits on the allowed mass range and interaction strength. This makes it interesting to look at alternative options.

- **Sterile neutrinos** are the subject of this thesis. They differ from the previous category because they are sterile, meaning that they only interact with other particles through gravitation.[4] They are introduced in the type-I seesaw model to generate masses for the active neutrinos. Their own masses are also a lot less constrained than WIMP masses, and can range from light (1 eV) to incredibly heavy (10^{15} GeV) [6][7].

[3]For comparison, the top quark is the heaviest particle in the SM at roughly 173 GeV. WIMP DM could be about 100 times heavier.

[4]We will see that they do have supressed interactions with the weak force because the active neutrino flavour eigenstates can mix with the sterile neutrinos to form the actual mass eigenstates.

3. Neutrino Physics

3.1 The Standard Model

The SM gives an overview of the known elementary particles and their properties, like electrical charge, colour charge and spin. We usually group the particles together based on these properties. *Fermions* are particles with half integer spin ($\frac{1}{2}$, $\frac{3}{2}$, etc) and *bosons* have integer spins. The bosons of the SM can be split up in gauge bosons with spin 1 and scalar bosons with spin 0. It is the gauge bosons that transmit the fundamental forces in particle interactions. The photon for the electromagnetic force, the gluons for the strong force and the Z^0- and $W^{\pm}$ bosons for the weak force. The Higgs particle is the only scalar boson in the SM. It is a remnant of the Higgs mechanism that is responsible for generating masses for the massive particles in the SM [8]. All fermions also have an associated antiparticle version. These have the same mass as their normal variant but their charges (electric charge, hypercharge) have opposite signs.[1] It is possible for a fermionic particle to be its own antiparticle if it carries no charges. These are known as Majorana particles. Neutrinos could be Majorana particles, but this is still an open question.

The fermions are further divided into quarks and leptons. Quarks posses a colour charge, which lets them participate in strong interactions. Leptons do not carry colour and do not feel the strong force. Both quarks and leptons exist in six flavours, and we order the flavours into three generations based on their mass. The particles of the first generation are the lightest, those of the third generation are the heaviest. Neutrinos fall into the lepton sector.

Table 3.1: The Lepton Sector of the SM

Generation	Flavour	Charge
First	e electron	-1
	ν_e electron neutrino	0
Second	μ muon	-1
	ν_μ muon neutrino	0
Third	τ tau	-1
	ν_τ tau neutrino	0

We see that we have three electrically charged leptons, the electron, muon and tauon, and three neutral ones, which are the corresponding neutrinos.

[1] As an exception, the $W^{\pm}$-bosons also have each other as their own antiparticles.

The neutrinos have no electrical or color charge, which means that they can only feel the weak force. This is interesting in the context of DM, since we know that WIMPS only interact weakly, and they are possible DM candidates. The problem is that neutrinos are too light to produce a large enough relic density. Historically neutrinos were thought to be massless. This is reflected in the original formulation of the SM, which does not assign masses to them. We now know from the observation of neutrino oscillations that neutrinos do have mass, albeit small compared to other fermions in their generations. Their exact masses are not known, but upper bounds have been determined by several experiments, with $m_{\nu_\mu} < 190$ keV and $m_{\nu_\tau} < 18.2$ MeV [9].

3.1.1 Chirality

Another property of fermions is their chirality. Fermionic particles can come in a left-handed or a right-handed chirality, which can be thought of as mirror images of each other. Chirality is related to the concept of helicity, which also divides particles into left- and right-handed categories, but these concepts are not exactly the same. A particle's helicity is right-handed when the spin of the particle is aligned with the direction of its motion and left-handed if its spin points the other way. For a massive particle helicity is not Lorentz invariant, since we can apply a lorentz boost to move to a new reference frame where the direction of the particle's velocity is reversed but the spin is unchanged, thus flipping its helicity. We cannot do this for a massless particle travelling at the speed of light, since no change of reference frame can reverse its velocity. Chirality is Lorentz invariant and for a massless particle it is equal to its helicity.

Interactions that only involve the strong and electromagnitic force are parity symmetric. This means that if we 'mirror' a particle event, replacing all involved particles with their counterpart of opposite chirality, the process is unchanged and the mirrored versions occur at equal probabilities. This is not the case for interactions involving the weak force. The weak force only couples to particles of left-handed chirality and antiparticles of right-handed chirality. So interactions mediated by the weak force, such as beta decay, only produce left-handed particles and right-handed antiparticles. The mirrored version does not occur.[2] Since neutrinos only participate in weak interactions, the original SM only includes left-handed neutrinos and right-handed antineutrinos. Right-handed neutrinos have not directly been observed as of yet. The other fermions do come in right- and left-handed versions that can be observed through SM interactions.

3.1.2 QFT and the Lagrangian

For now we will accept that the neutrinos have mass, and will refrain from altering the SM. This is left for the next chapter, where we introduce the type-I seesaw mechanism. But in order to do so we will have to lift the hood on the SM a bit

[2]Technically this is only true for the so called 'charged current' weak interactions that couple with the the $W^\pm$ bosons. The Z^0-boson can couple to right-handed particles, but the interaction strength is still not conserved under parity transformations.

further and take a glimpse at the underlying mathematics.

The SM is a quantum field theory (QFT) [10]. In QFT particles are not treated as point-like but as excitations of an underlying quantum field. We also impose a symmetry on the SM. It is invariant under local $SU(3)_C \otimes SU(2)_L \otimes U(1)_Y$ transformations. These are Lie groups, and each is associated with certain conserved charges. The only thing we need to know for now is that under these transformations the SM (or parts of it) must remain invariant, very similar to the concepts of parity symmetry and 'mirroring' described in the previous section.

The way the fields of the SM interact is defined in its Lagrangian $\mathcal{L}$. The Lagrangian contains terms that we can split up in sectors: the strong sector (or QCD sector, for Quantum Chromo Dynamics) that obeys the $SU(3)$ group symmetry, the electroweak sector, that combines electromagnetic and weak interactions and obeys $SU(2) \otimes U(1)$ symmetry, and the Higgs and Yukawa sectors that are both concerned with generating particle masses. Mass terms for fermions in the SM Lagrangian need both left-handed and right-handed particle fields. These couple to the Higgs field through so called Yukawa interactions to generate the mass terms. For charged leptons the mass terms take the form [11]:

$$-\mathcal{L}_{mass}^{Dirac} = \overline{\psi}_L m_D \psi_R + \overline{\psi}_R m_D^\dagger \psi_L \tag{3.1}$$

Here ψ_L are left-handed lepton fields and ψ_R the right-handed ones. The object m_D is a mass matrix, and it is the product of a Yukawa matrix and the vacuum expectation value of the Higgs.

We can not construct such a mass term for neutrinos in the original SM because it only includes left-handed neutrino fields. We are missing the right-handed fields that are also necessary. Now, for Majorana particles, we can write a mass term that uses only left-handed or right-handed fields. The problem is that such a Majorana mass term for the neutrinos with only left-handed fields would break the local $SU(2)$ invariance of the SM and is therefore not allowed. So we are left without mass terms for neutrinos in this minimal formulation of the SM.

3.2 Oscillations

The first experimental evidence for neutrino mass was found in the Homestake experiment, that started in 1968 [9]. In spite of the small interaction cross section of neutrinos with atomic nuclei, they were able to detect electron neutrinos produced in the sun with a large underground detector. They found that the number of electron neutrinos they captured was roughly a third of what was expected based on the solar model for neutrino production.

A theoretical explanation for this lack of electron neutrinos already existed. In 1958 Bruno Pontecorvo proposed that neutrinos could have a small mass, and undergo oscillations [9]. This means that a neutrino that is produced in charged current weak interactions as a certain flavour, has a probability that when it is measured some distance from the source it will have changed to a different neutrino flavour. It

is referred to as oscillations because the probability of a neutrino switching flavour oscillates as a function of the distance travelled from its source. An electron neutrino produced in the sun through fusion reactions has a probability to be measured on earth as a muon- or tau neutrino. The Homestake experiment was not sensitive to those, and these oscillations would suppress the total electron neutrino flux reaching earth from the sun.

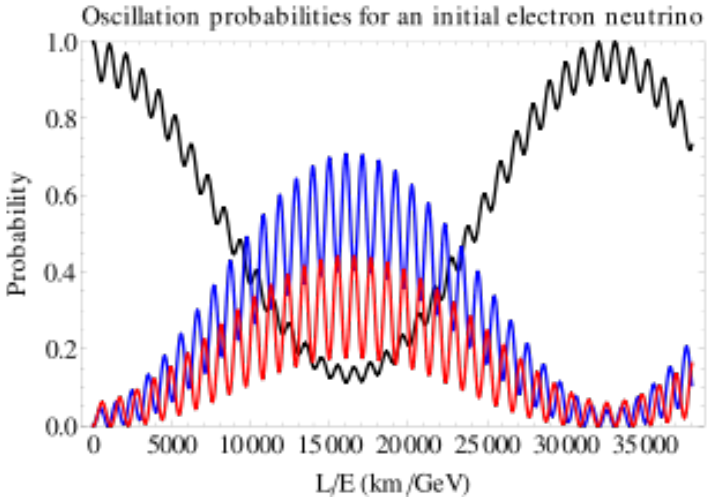

Figure 3.1: Neutrino oscillations of an initial electron neutrino at some distance from its source. The black line is the probability of measuring a electron neutrino, the blue line for measuring a muon neutrino and the red line for measuring a tau neutrino [12].

Neutrinos are produced in weak interactions at an interaction point (vertex) with a W-boson and a charged lepton. The neutrino and charged lepton are created at the vertex as flavour eigenstates of the same generation. But, now that we are working with neutrinos that have a mass, the neutrinos are not necessarily created as mass eigenstates [11]. We will call the mass eigenstates ν_1, ν_2 and ν_3.

We can express a flavour-eigenstate electron neutrino at the time of its creation as a linear superposition of the three mass eigenstates. $|\nu(0)\rangle = |\nu_e\rangle = a\,|\nu_1\rangle + b\,|\nu_2\rangle + c\,|\nu_3\rangle$. More generally, for $\nu_\alpha,\ \alpha = e, \mu, \tau$ and for $\nu_j,\ j = 1, 2, 3$ (We will be using Greek indices for flavour eigenstates and Latin indices for the mass eigenstates):

$$|\nu(0)\rangle = |\nu_\alpha\rangle = \sum_j U^*_{\alpha j}\,|\nu_j\rangle \tag{3.2}$$

U is a complex unitary matrix ($U^\dagger U = I$). It contains the information of how the mass eigenstates mix to form flavour eigenstates (and vice versa). It is known as the Pontecorvo-Maki-Nakagawa-Sakata (PMNS) matrix.

If we want to know how the mass eigenstates evolve with time we have to solve for the (time dependent) schrödinger equation: $i\frac{d}{dt}\,|\Psi(t)\rangle = \hat{H}\,|\Psi(t)\rangle$.[3] Since the $|\nu_j\rangle$ states are mass (energy) eigenstates we simply pick up a phase factor $e^{-iE_j t}$:

[3]We use natural units, $\hbar = c = 1$

$$|\nu(t)\rangle = \sum_j U^*_{\alpha j} e^{-iE_j t} |\nu_j\rangle \tag{3.3}$$

The phase factor is what causes the oscillations. Since the three mass eigenstates each have a different E_j in their phase factors, the probability of finding a neutrino in a different flavour eigenstate at time $t > 0$ is nonzero. We can calculate the probability of these transitions. Using that the mass eigenstates are mutually orthogonal and normalized:

$$\begin{aligned} A(\nu_\alpha \to \nu_\beta; t) &= \langle \nu_\beta | \nu(t) \rangle \\ &= \sum_{j,k} (U_{\beta k} \langle \nu_k |)(e^{-iE_j t} U^*_{\alpha j} |\nu_j\rangle) \\ &= \sum_{j,k} U_{\beta k} U^*_{\alpha j} e^{-iE_j t} \langle \nu_k | \nu_j \rangle \\ &= \sum_j U_{\beta j} U^*_{\alpha j} e^{-iE_j t} \\ P(\nu_\alpha \to \nu_\beta; t) = |A|^2 &= |\sum_j U_{\beta j} U^*_{\alpha j} e^{-iE_j t}|^2 \end{aligned} \tag{3.4}$$

So, the probability P is not zero and the complex phases describing the time evolution of the mass eigenstates lead to the oscillatory behaviour.

3.2.1 The Parameters

To understand the transition probability P in more detail we want to know the structure of the PMNS matrix. Right now the only thing we have stated is that it is complex and unitary. We will take a look at its degrees of freedom and its standard representation.

A general complex $n \times n$ matrix has n^2 entries, and each entry has a real and a complex part, giving us $2n^2$ parameters. Unitarity, $U^\dagger U = I$, gives us a set of n^2 equations [4]. Thus reducing the number of free parameters down to n^2. We will divide these into $\frac{n(n-1)}{2}$ parameters in the form of mixing angles θ and $\frac{n(n+1)}{2}$ parameters in the form of complex phases $e^{i\phi}$.

Since we have three neutrinos that means we are working with three mixing angles $(\theta_{12}, \theta_{13}, \theta_{23})$ and six phases. We can use a little trick to reduce the number of complex phases. It is possible to redefine the flavour and mass eigenstates by multiplying them with a complex phase factor without changing their physics. We can move the complex phases from one row of the PMNS matrix to the definition of the mass eigenstates and of one column to the definition of the flavour eigenstates.[5] This reduces the number of complex phases by $2n - 1$, so in the end for our $n = 3$

[4] one for each entry of $U^\dagger U$, setting it to 1 on the diagonal and 0 on the off-diagonal entries

[5] If the neutrinos are Majorana particles (being their own antiparticle) we can't rephase the mass eigenstates and can only remove n phases from the PMNS matrix. In this case it does not matter, since the extra 'Majorana phases' present do not have an effect on oscillation

case we are left with three mixing angles and one complex phase. The PMNS matrix is parameterized as:

$$
\begin{aligned}
U &= \begin{pmatrix} 1 & 0 & 0 \\ 0 & c_{23} & s_{23} \\ 0 & -s_{23} & c_{23} \end{pmatrix} \begin{pmatrix} c_{13} & 0 & s_{13}e^{-i\delta_{CP}} \\ 0 & 1 & 0 \\ -s_{13}e^{i\delta_{CP}} & 0 & c_{13} \end{pmatrix} \begin{pmatrix} c_{12} & s_{12} & 0 \\ -s_{12} & c_{12} & 0 \\ 0 & 0 & 1 \end{pmatrix} \\
&= \begin{pmatrix} c_{12}c_{13} & s_{12}c_{13} & s_{13}e^{-i\delta_{CP}} \\ -s_{12}c_{23} - c_{12}s_{13}s_{23}e^{i\delta_{CP}} & c_{12}c_{23} - s_{12}s_{13}s_{23}e^{i\delta_{CP}} & c_{13}s_{23} \\ s_{12}s_{23} - c_{12}s_{13}c_{23}e^{i\delta_{CP}} & -c_{12}s_{23} - s_{12}s_{13}c_{23}e^{i\delta_{CP}} & c_{13}c_{23} \end{pmatrix}
\end{aligned} \tag{3.5}
$$

where $c_{ij} = \cos(\theta_{ij})$ and $s_{ij} = \sin(\theta_{ij})$.

We see three rotation matrices with an added complex phase factor. The PMNS matrix rotates the base of the flavour space into the base spanned by the mass eigenstates. This rotation is paired with a complex phase shift.
With the PMNS matrix parameterised we can calculate the probability in equation (3.4). We will make two additional assumptions. First, for neutrinos travelling almost at the speed of light $t \approx L$, where L is the distance travelled from the source. Second, we expand the energy associated with ν_j; $E_j = \sqrt{\vec{p}^2 + m_j^2} \simeq |\vec{p}| + \frac{m_j^2}{2|\vec{p}|} \simeq |\vec{p}| + \frac{m_j^2}{2E}$. The probability function now becomes:

$$
\begin{aligned}
P(\nu_\alpha \to \nu_\beta) &= |\sum_j U_{\beta j} U^*_{\alpha j} e^{-i m_j^2 \frac{L}{2E}}|^2 \\
&= \sum_{j=1}^{3} |U_{\beta j}|^2 |U_{\alpha j}|^2 \\
&+ \sum_{j<k} 2\mathrm{Re}[U_{\beta j} U^*_{\beta k} U^*_{\alpha j} U_{\alpha k}] \cos \frac{\Delta m^2_{jk} L}{2E} \\
&+ \sum_{j<k} 2\mathrm{Im}[U_{\beta j} U^*_{\beta k} U^*_{\alpha j} U_{\alpha k}] \sin \frac{\Delta m^2_{jk} L}{2E}
\end{aligned} \tag{3.6}
$$

where $\Delta m^2_{jk} = m_j^2 - m_k^2$.
Thus experiments that look at neutrino oscillations are sensitive to the parameters of the PMNS matrix (the mixing angles θ_{ij} and the complex phase δ_{CP}) and the difference of the squared neutrino masses.

3.2.2 Values and Ordering

There have been many experiments working to determine the parameters involved with neutrino oscillations. Fig 3.2. gives a recent overview of global results. Because of the difficulty in detecting neutrinos there are still reasonably large uncertainties in these parameters.

The table is split up into two versions, one for normal ordering and one for inverse ordering (also referred to as normal and inverse hierarchy). This is because the

Table 3.2: Values for the neutrino oscillation parameters. Fit to global data available as of July 2020 [13].

	Normal Ordering (best fit)		Inverted Ordering ($\Delta\chi^2 = 2.7$)	
	bfp $\pm 1\sigma$	3σ range	bfp $\pm 1\sigma$	3σ range
$\sin^2\theta_{12}$	$0.304^{+0.013}_{-0.012}$	$0.269 \to 0.343$	$0.304^{+0.013}_{-0.012}$	$0.269 \to 0.343$
$\theta_{12}/^\circ$	$33.44^{+0.78}_{-0.75}$	$31.27 \to 35.86$	$33.45^{+0.78}_{-0.75}$	$31.27 \to 35.87$
$\sin^2\theta_{23}$	$0.570^{+0.018}_{-0.024}$	$0.407 \to 0.618$	$0.575^{+0.017}_{-0.021}$	$0.411 \to 0.621$
$\theta_{23}/^\circ$	$49.0^{+1.1}_{-1.4}$	$39.6 \to 51.8$	$49.3^{+1.0}_{-1.2}$	$39.9 \to 52.0$
$\sin^2\theta_{13}$	$0.02221^{+0.00068}_{-0.00062}$	$0.02034 \to 0.02430$	$0.02240^{+0.00062}_{-0.00062}$	$0.02053 \to 0.02436$
$\theta_{13}/^\circ$	$8.57^{+0.13}_{-0.12}$	$8.20 \to 8.97$	$8.61^{+0.12}_{-0.12}$	$8.24 \to 8.98$
$\delta_{\rm CP}/^\circ$	195^{+51}_{-25}	$107 \to 403$	286^{+27}_{-32}	$192 \to 360$
$\frac{\Delta m^2_{21}}{10^{-5}\ \mathrm{eV}^2}$	$7.42^{+0.21}_{-0.20}$	$6.82 \to 8.04$	$7.42^{+0.21}_{-0.20}$	$6.82 \to 8.04$
$\frac{\Delta m^2_{3\ell}}{10^{-3}\ \mathrm{eV}^2}$	$+2.514^{+0.028}_{-0.027}$	$+2.431 \to +2.598$	$-2.497^{+0.028}_{-0.028}$	$-2.583 \to -2.412$

experiments are only sensitive to the absolute squared mass differences Δm^2_{jk} of the neutrinos, and not their absolute mass. For three neutrinos there are two mass splittings, and experiments have found one to be several orders larger than the other. We do not know if the small mass splitting is between the two lightest neutrinos (normal ordering) or if it is between the heavy neutrinos (inverse ordering). Notably, it is possible for the lightest mass eigenstate to be zero, since we only know upper bounds for the neutrino masses and we can only measure the two mass splittings.

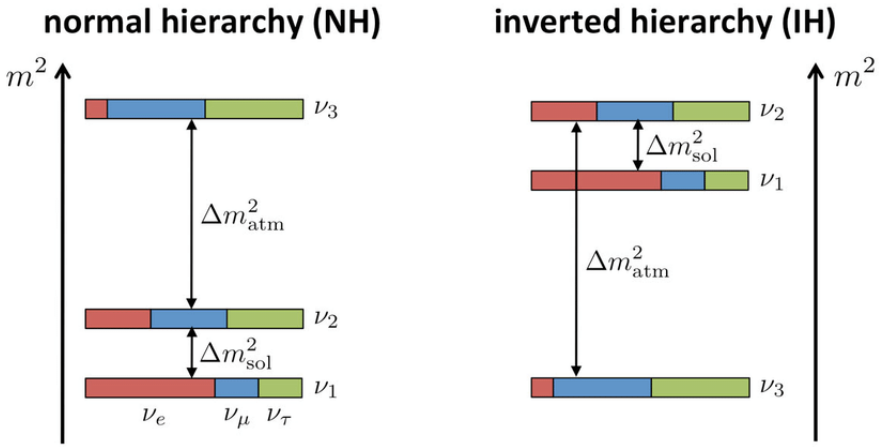

Figure 3.2: The two possible orderings of the neutrino masses. The colours indicate the mixing of the flavour eigenstates for each mass eigenstate. Δm^2_{sol} refers to the transition from electron to muon neutrinos between the sun and earth. Δm^2_{atm} refers to muon neutrinos, that are produced by cosmic rays in the earths atmosphere, transitioning to tau neutinos [14].

4. the Type-I Seesaw Mechanism

The type-I seesaw mechanism explains both the existence of neutrino mass, and their relative smallness compared to the other fermions in their generation.[1] This is done by introducing new heavy, right-handed neutrinos to the SM. Because of their right-handedness they do not couple to the weak force like the left-handed (active) light neutrinos do. The presence of right-handed neutrinos makes it possible to construct neutrino mass terms in the SM Lagrangian, and they suppress the mass of the active neutrinos with their own heavy masses. This interplay between the masses of the sterile and active neutrinos is what gives the seesaw mechanism its name. Increasing the mass of the sterile neutrinos decreases the mass of the active ones, like a seesaw going up and down. For every right-handed neutrino we add to the SM we can generate mass for one active neutrino. To reproduce the correct mass-splittings Δm^2_{ij} we need at least two sterile neutrinos to provide mass to two active neutrinos.

We saw that it is not possible to have a mass term with two left-handed particle fields in the Lagrangian. Now that we have access to right-handed neutrinos we can construct a Dirac mass term.[11]:

$$-\mathcal{L}^{Dirac}_{mass} = \overline{\psi}_L m_D \psi_R + \overline{\psi}_R m_D^\dagger \psi_L \tag{4.1}$$

As of yet it is unclear whether neutrinos are Dirac or Majorana particles. Majorana particles are particles which are their own antiparticles, which is possible for neutrinos because they don't carry charges. We have the possibility to construct a Majorana[2] mass term, which is constructed with only right-handed or only left-handed fields. We could not use two left-handed fields because it breaks the local symmetry of the SM, but we have more freedom with the right-handed neutrinos since they do not need to transform under the $SU(2) \times U(1)$ symmetry of the electroweak sector [1]:

$$-\mathcal{L}^{Majorana}_{mass} = \frac{1}{2}(\overline{\psi^c}_R M_M \psi_R) + h.c. \tag{4.2}$$

Here we use the charge conjugated field $\overline{\psi^c}_R$. Charge conjugation replaces the particle with its corresponding antiparticle and changes its chirality. These two mass

[1] Additionally there are also the type-II and type-III seesaw mechanisms. Instead of adding right-handed neutrino fields to the SM they respectively add a boson and fermion triplet to the SM. [15]

[2] Proof of the Majorana nature of neutrinos would be the observation of neutrinoless double beta decay, where two neutrons simultaneously decay and emit an electron and a (anti)neutrino. If the neutrino is Majorana these two decays can 'share' one (anti)neutrino for both processes. In the final state there will only be two protons, two electrons and no (anti)neutrino.

terms together describe the neutrino masses in this extension of the SM. We can combine them into one expression. Replacing the general fermionic fields ψ with neutrino fields ν we get:

$$-\mathcal{L}_{M_\nu} = \frac{1}{2}\begin{pmatrix}\bar{\nu_L} & \bar{\nu_R^c}\end{pmatrix}\begin{pmatrix}0 & m_D\\ m_D^T & M_M\end{pmatrix}\begin{pmatrix}\nu_L^c\\ \nu_R\end{pmatrix} + h.c. \equiv \frac{1}{2}\begin{pmatrix}\bar{\nu_L} & \bar{\nu_R^c}\end{pmatrix} M \begin{pmatrix}\nu_L^c\\ \nu_R\end{pmatrix} + h.c. \quad (4.3)$$

We will call M the neutrino mass matrix. It is constructed from submatrices, the $3 \times n_s$ Dirac mass matrix m_D and the symmetric $n_s \times n_s$ Majorana mass matrix M_M, where n_s is the number of sterile neutrinos added to the SM. We can (block-)diagonalize the mass matrix with a unitary matrix U [6]:

$$U^\dagger \cdot M \cdot U^* = \begin{pmatrix}M_1 & 0\\ 0 & M_2\end{pmatrix} \quad (4.4)$$

After diagonalisation M_1 is the effective mass matrix for the active neutrinos and M_2 for the sterile neutrinos. We want to find expressions for the matrices M_1 and M_2 by solving the characteristic equation of mass matrix M:

$$\det(M - \lambda I) = \det\begin{pmatrix}-\lambda I_3 & m_D\\ m_D^T & M_M - \lambda I_{n_s}\end{pmatrix} = 0 \quad (4.5)$$

Where I_n is the n-dimensional identity matrix. For the determinant of a block matrix we have [16]:

$$\det\begin{pmatrix}\mathbf{A} & \mathbf{B}\\ \mathbf{C} & \mathbf{D}\end{pmatrix} = \det(\mathbf{A} - \mathbf{B}\mathbf{D}^{-1}\mathbf{C})\det(\mathbf{D}) \quad (4.6)$$

Here $\mathbf{A}$ and $\mathbf{D}$ are square matrices, and $\mathbf{D}$ must be invertible. This means that we have to be careful that $M_M - \lambda I_{n_s}$ is an invertible matrix (and thus that its determinant is non-zero).

$$\det\begin{pmatrix}-\lambda I_3 & m_D\\ m_D^T & M_M - \lambda I_{n_s}\end{pmatrix} = \det\left(-\lambda I_3 - m_D(M_M - \lambda I_{n_s})^{-1} m_D^T\right)\det\left(M_M - \lambda I_{n_s}\right) = 0$$

$$\Rightarrow \det\left(-\lambda I_3 - m_D(M_M - \lambda I_{n_s})^{-1} m_D^T\right) \overset{\lambda \ll M_M}{\simeq} \det\left(-m_D M_M^{-1} m_D^T - \lambda I_3\right) = 0$$

$$\det\left(M_M - \lambda I_{n_s}\right) \simeq 0$$

$$\Rightarrow M_1 \simeq -m_D M_M^{-1} m_D^T \quad (4.7)$$

$$M_2 \simeq M_M \quad (4.8)$$

The characteristic equation of M is approximately the product of two characteristic equations for the matrices $-m_D M_M^{-1} m_D^T$ and M_M, which correspond to M_1 and M_2. This is where we see the seesaw behaviour of the system, the values of M_1 (and thus the masses of the active neutrinos) are suppressed by a factor M_M^{-1}, while the values of M_2 scale linearly with M_M. To get this result we made use of the seesaw limit $\lambda \ll M_M$. In practice this limit holds well for a large range of values for M_M, ranging from 1 eV to 10^{15} GeV [6].

We used the matrix U to diagonalize the neutrino mass matrix. It serves as the mixing matrix for the mass and flavour eigenstates of the collection of active and sterile neutrinos.

$$\nu_\alpha = U_{\alpha i}\nu_i,\ \nu_i = U^*_{\alpha i}\nu_\alpha \tag{4.9}$$
$$\text{where } \alpha = e, \mu, \tau, s_1, ..., s_{n_s},\ i = 1, 2, 3, ..., n_s + 3$$

Importantly the process of neutrino oscillations set up in section 3.2 also applies here. The sterile and active neutrino flavour eigenstates can mix in the mass eigenstates, and oscillations between active and sterile neutrinos are possible. Mixing opens up the possibility for sterile neutrinos to participate in weak interactions, since the active neutrino flavour states contribute to the heavy mass eigenstates. We can define a mixing matrix between sterile and active neutrinos as [17]:

$$\theta = m_D M_M^{-1} \tag{4.10}$$

We can see that the mixing is suppressed for large Majorana masses. Stronger mixing is possible if we choose one (or more) of the heavy neutrino mass eigenstates to lie closer to the light mass eigenstates $\nu_{1,2,3}$. Mixing between active and sterile states may be an explanation for what is known as the reactor anomaly. Neutrino detectors placed at ≤ 100 m from nuclear reactors measure an approximately 5% [18] smaller neutrino flux then the reactor is expected to produce. This could be due to oscillations to sterile neutrino states [9].

5. Data and Results

5.1 Method

Now that we have set up the type-I seesaw mechanism as our model for generating neutrino masses we can do a search of its parameter space. The seesaw mechanism introduces new parameters to the SM in the form of the entries of the Dirac and (symmetric) Majorana mass matrices. Their size depends on the number of right-handed neutrinos added to the SM. We choose to add three, in order to provide mass to all three active neutrinos. We refer to this as a 3+3 mass model. We must also make choices about: What information we are interested in extracting from the model, what tools and methods to use to get this information, and over what ranges we are going to search the entries of the Dirac and Majorana mass matrices. We want to address three questions:

- What do the distributions of the mass eigenvalues of mass matrix M look like, and can we reproduce the mass splittings of the active neutrinos found in table 3.2? We can find the masses by calculating the eigenvalues of $M_1 \simeq -m_D M_M^{-1} m_D^T$ and $M_2 \simeq M_M$. We order them from heaviest (m_{ν_6}) to lightest (m_{ν_1}).

- What will be the mixing of the mass eigenstates in terms of flavour eigenstates? We mainly want to know how strong the sterile neutrinos can contribute to the light mass eigenstates. The mixing matrix U diagonalizes the neutrino mass matrix M, so we can construct it by inserting the eigenvectors of M as the columns of U .

- How do these results relate to the possibility of sterile neutrino DM? What are the constraints on sterile neutrino DM and has our parameter search delivered any suitable solutions?

The type-I seesaw model does not directly place any restrictions on the structure of the Majorana and Dirac matrices, other than that the Majorana mass matrix is symmetric. For convenience and to reduce the number of free parameters we also choose m_D to be symmetric:

$$m_D = \begin{pmatrix} a & b & c \\ b & d & e \\ c & e & f \end{pmatrix}, \; M_M = \begin{pmatrix} g & h & i \\ h & j & k \\ i & k & l \end{pmatrix} \tag{5.1}$$

In total M has twelve free parameters. The only limit on the values we can choose for the parameters comes from the seesaw limit $m_D \ll M_M$. We choose to sample points

uniformly in the ranges $\{a, b, ..., f\} \in [0 - 1 \cdot 10^3\,\text{eV}]$ and $\{g, h, .., l\} \in [0 - 1 \cdot 10^9\,\text{eV}]$.[1] With these assumptions in place we generate $\mathcal{O}(10^6)$ neutrino mass matrices and calculate their mass eigenvalues and mixing matrices.

5.2 Mass

Figure 5.1 shows the distributions of the three light and three heavy neutrino masses. We see a clear distinction in mass of up to 13 orders of magnitude between the the three heavy and three light neutrinos, as we expect from the seesaw mechanism. Within the light and heavy sectors we see that the distributions get progressively wider for higher mass eigenstates, and each has its own distinct peak. Negative masses are allowed; the absolute value is the actual physical quantity. We plot the masses as negative in the histograms to show that there is an asymmetry between the generated positive and negative values. The bias towards negative eigenvalues is expected because of the sign of formula 4.7.The masses for ν_2, ν_3 and ν_5 have dips around $m = 0$ eV, since this is the range where the lightest heavy and light mass eigenstates ν_1 and ν_4 have their mass eigenvalues. Only the distribution of the heaviest mass eigenstate ν_6 is not centered around $m = 0$ eV.

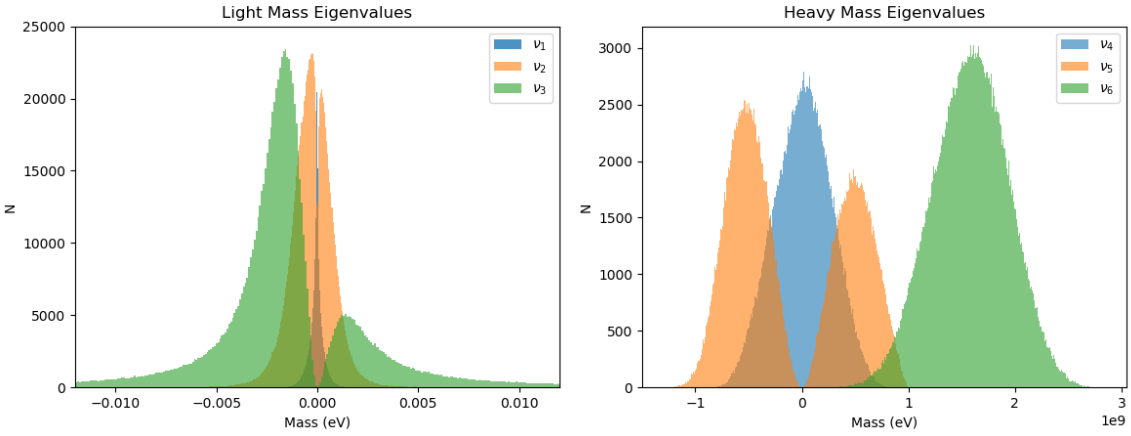

Figure 5.1: Histograms of the eigenvalues of neutrino mass matrix M. Left: light neutrino masses m_{ν_1}, m_{ν_2} and m_{ν_3}. Right: heavy neutrino masses m_{ν_4}, m_{ν_5} and m_{ν_6}. Number of bins = 1000.

We can check if any of the generated data points produces light neutrinos that are consistent with experimental constraints. The generated masses easily fall below the upper mass bounds $m_{\nu_e} < 1\,\text{eV}, m_{\nu_\mu} < 190\,\text{keV}$ and $m_{\nu_\tau} < 18.2$ MeV [9]. However, when we impose the constraints on Δm^2_{ij} found in table 3.2, we find exactly

[1]The Majorana mass is not as bounded as this search range suggests. Earlier we stated that it can be as large as 10^{15} GeV. We choose this range because of technical limitations. To find M_1 we need to calculate the inverse of M_M. This calculation is done in Python, using the matrix inverse function of the numpy package. This is an iterative function with limited precision output, and for entries of M_M higher than the chosen range the calculation is not precise enough. This leads to unreliable values for the neutrino masses.

one point that falls within the 3σ range for the normal ordering scenario and none for inverse ordering. If we relax the constraints by only demanding that the ratio $\frac{\Delta m^2_{21}}{\Delta m^2_{32}}$ is within 3σ-confidence we find 32313 data points with the correct ratio for normal ordering and 837 points for inverse ordering. This shows that this uniform parameter search is not optimal for finding specific points within the model. We are working with a large parameter space and we scan over a large range of values for the M_M entries. Further research could focus on ways to increase the number of physical points found in a search. For example by specifically searching in the neighbourhood of our 'correct' point (using that point as a seed) or using non-uniform distributions to generate entries for the mass matrix.

5.3 Mixing

The entries of the mixing matrix tell us how the mass eigenstates are decomposed in terms the flavour eigenstates: $U^*_{\alpha i}\nu_\alpha = \nu_i$. We can visualize the relationship between the mass eigenstates and the mixing of specific flavours in scatter plots. With six mass eigenstates and 6×6 matrix elements there are 216 total plots. We will show a small selection to illustrate possible behaviour of the model. Figure 5.2 shows the composition breakdown of mass eigenstate ν_4, the lightest of the heavy neutrinos, as functions of the ν_4 mass eigenvalues. Figure 5.3 shows the same but for the heaviest of the light neutrinos ν_3. We choose these mass eigenstates because they respectively show the strongest mixing of active neutrino flavour eigenstates in heavy mass eigenstates and sterile flavour eigenstates in the light mass eigenstates.

For plots of all six mass eigenstates see appendix A. In figure 5.2 we see that the active neutrino flavour states can contribute to mass eigenstate ν_4, but only when the ν_4 mass approaches the light neutrino mass range. This results in these cross-shaped plots, where all points with non-zero mixing have small masses and appear to lie on a horizontal line (in reality there is some variation in their masses).The mass eigenstate ν_5 shows the same behaviour, but due to its higher masses the mixing is much weaker, whereas ν_6 has almost no mixing with the active neutrino states. The mixing of the sterile neutrino states is largely unconstrained, even allowing ν_4 to be a (nearly) pure flavour eigenstate (where the mixing of a certain flavour eigenstate equals 1). Whenever the absolute mixing of a flavour eigenstate exceeds $\sqrt{\frac{1}{2}}$, it is automatically the flavour that contributes the most to the total mixing of the mass eigenstate. This leads to the monochromatic bands of points at the sides of the plots for the sterile neutrino flavours in figure 5.2, and for the active neutrinos in figure 5.3.

In figure 5.2 we see that for negative mass values the maximum allowed mixing of the sterile flavour states decreases. This is a result of our chosen parameter ranges. We have only allowed positive values for the entries of the Dirac and Majorana mass matrices. As a result we can only achieve negative mass eigenvalues through the mixing of multiple flavour eigenstates. This means that we need increasingly more mixing of flavour eigenstates to accomplish the lower negative mass eigenvalues, so the maximum allowed mixing of the individual flavour eigenstates decreases. We see the same effect for ν_5.

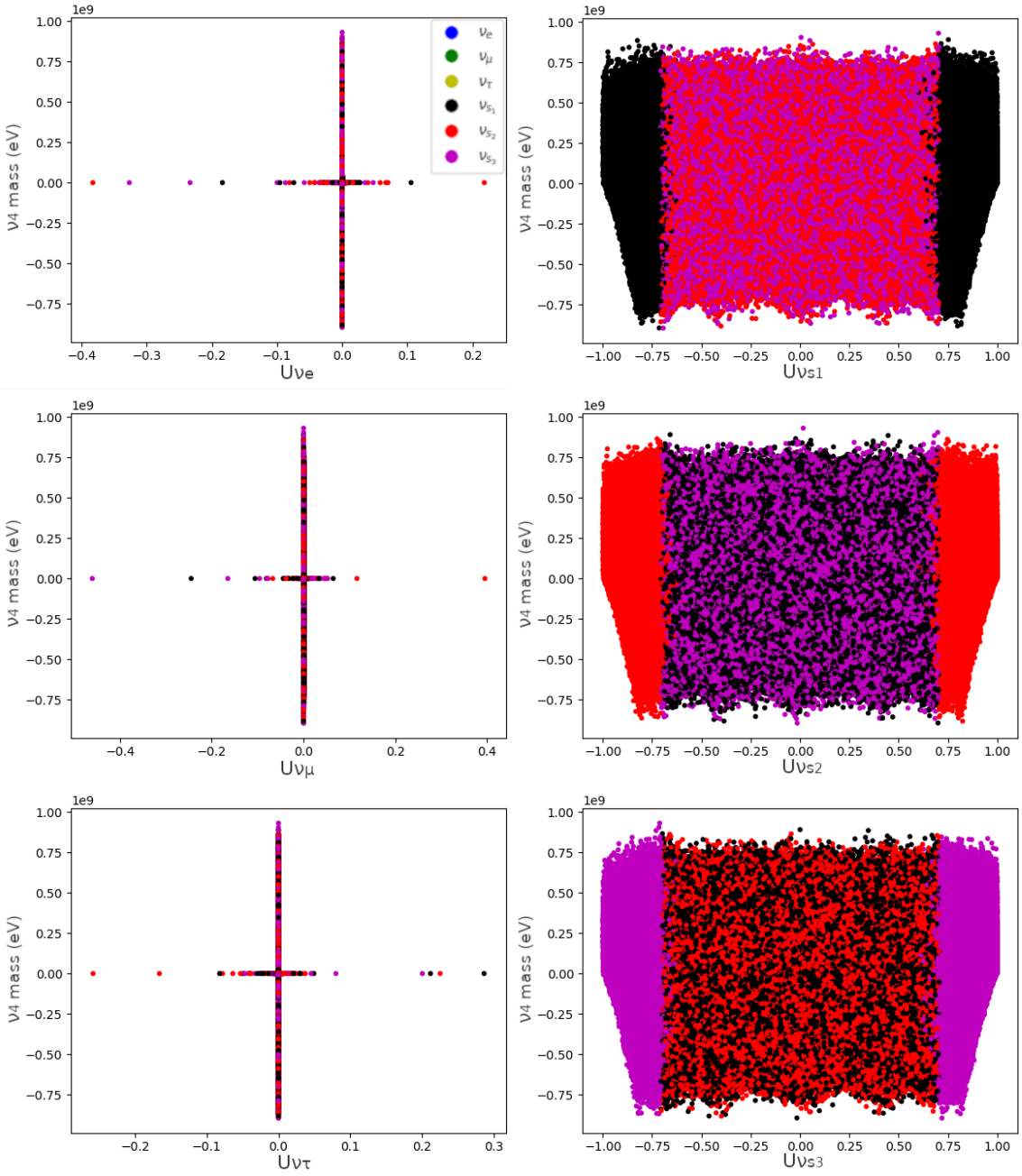

Figure 5.2: Scatter plots of the mixing strengths (given by the elements of the mixing matrix $U_{\alpha i}$) of the neutrino flavour eigenstates ν_α for mass eigenstate ν_4, plotted against the ν_4 mass. The colours indicate which of the flavour eigenstates contributes the most to the total ν_4 mixing for that data point. A mixing of $U = 0$ means that for that data point the flavour eigenstate does not contribute to the total mixing of ν_4. A mixing of 1 means that ν_4 is a pure flavour eigenstate.

Another effect of our chosen parameter range can be seen in the mixing of the sterile neutrino eigenstates for mass eigenstate ν_6 (See Fig. A.6 in appendix A). For masses larger than $1.0 \cdot 10^9$ eV, the maximum for the range of M_M, we see again that we need mixed mass eigenstates and thus we can no longer obtain pure flavour eigenstates. Additionally, when we pass two times the maximum parameter range, the

minimum allowed mixing of the sterile eigenstates starts increasing, and the maximum allowed mixing starts decreasing more sharply. This shows that we can only reach these mass values when all three sterile flavour eigenstates have significant presence in the total mixing.

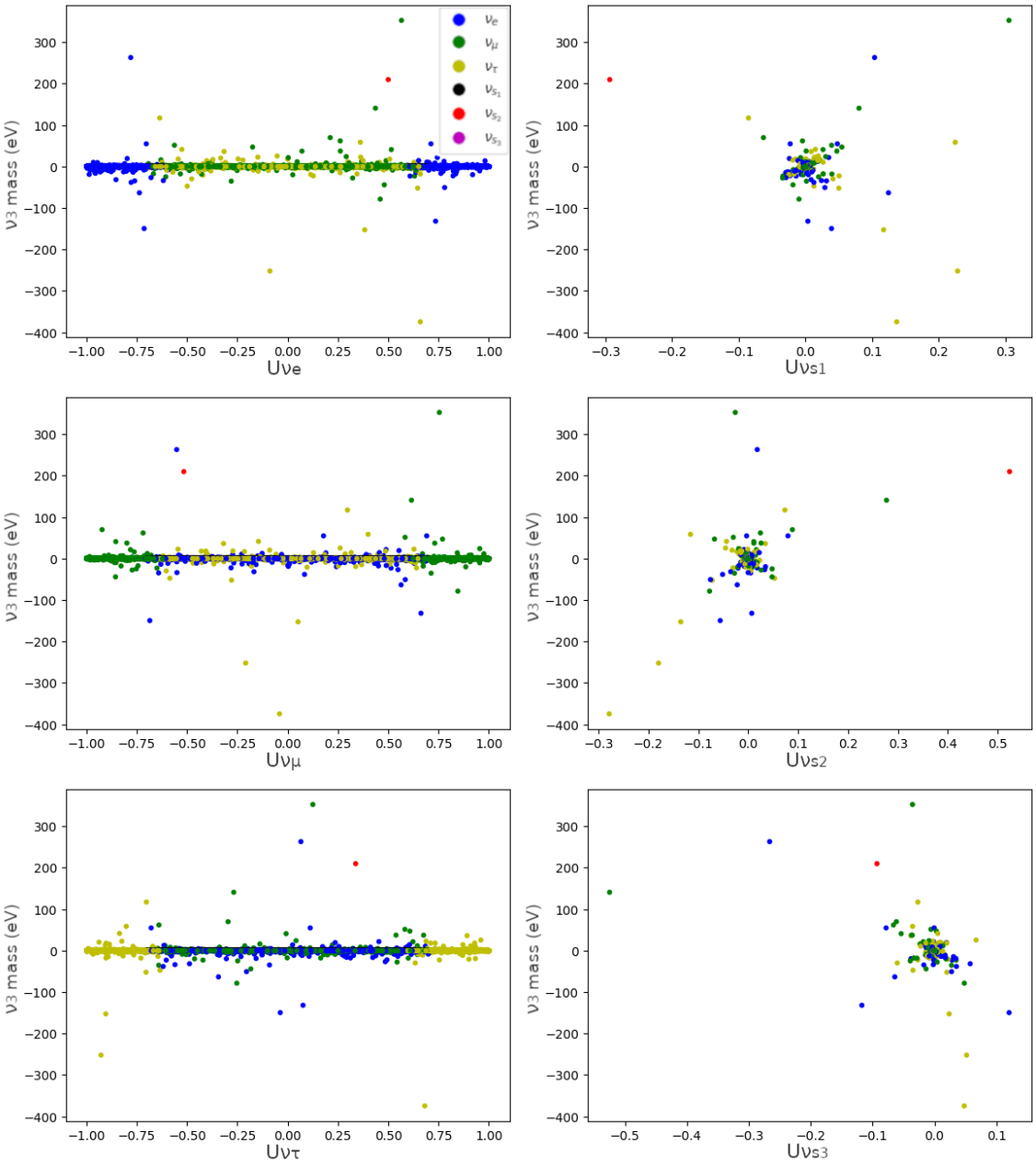

Figure 5.3: Scatter plots of the mixing strengths (given by the elements of the mixing matrix $U_{\alpha i}$) of the neutrino flavour eigenstates ν_α for mass eigenstate ν_3, plotted against the ν_3 mass. The colours indicate which of the flavour eigenstates contributes the most to the total ν_3 mixing for that data point. A mixing of $U = 0$ means that for that data point the flavour eigenstate does not contribute to the total mixing of ν_3. A mixing of 1 means that ν_3 is a pure flavour eigenstate.

In figure 5.3 we see that the contribution of the sterile neutrino states to ν_3 is mostly clumped in a neighbourhood around zero mass and zero mixing, but there are some

scattered points with stronger contributions from the sterile flavour eigenstates, and significantly higher possible mass eigenvalues (that were not visible in figure 5.1 since we truncated the tails of the distributions). We even have one point where ν_{s_2} provides the largest contribution to the total mixing. This behaviour differs strongly from ν_1 and ν_2, where we see almost no contribution of the sterile neutrino flavour states to the mixing, and no masses that exceed even 0.15 eV (see Appendix). That ν_3 has stronger contributions from the sterile flavour eigenstates is to be expected, since this mixing is what gives mass to the light neutrinos and ν_3 is the heaviest among them.

6. Sterile Neutrino Dark Matter

If we want to check that our parameter search has produced sterile neutrinos that are suitable DM candidates we need to understand what constraints exist on sterile neutrino DM in general. We will start referring to the sterile neutrino DM particle as N_1. We can use a combination of theoretical arguments and observational evidence to place limits on the mass of N_1 and the active-sterile mixing angle θ. From sources [1] and [19]:

- **Stability** Through the mixing of N_1 from the active neutrino states it is no longer stable and can decay via weak interactions. The dominant decay channel is $N_1 \to \nu_\alpha \nu_\beta \bar{\nu}_\beta$. DM candidates should have a half life longer than the age of the universe, which places an upper bound on the active-sterile mixing angle $\theta^2 \equiv \sum_{\alpha=e,\mu,\tau} |\theta_{\alpha 1}|^2 < 3.3 \times 10^{-4} \left(\frac{10\,\text{keV}}{M_{N_1}}\right)^5$.

- **X-ray bounds** Another more suppressed decay channel of the sterile neutrino is the radiative decay $N_1 \to \gamma \nu_\alpha$ (See figure 6.1). It predicts photons with an energy of half the sterile neutrino mass. These photons provide a potentially measurable signal from cosmic sterile neutrinos. We can exclude regions of allowed mass and mixing angle based on the absence of this signal in observations. These searches typically focus on sterile neutrino masses in the keV range. Interestingly there is an unexplained signal in X-ray spectra of some galaxy clusters, as well as in the Milky Way and Andromeda galaxies, at ~ 3.5 keV. This could be a signal from sterile neutrino DM with mass ~ 7 keV. This is not confirmed, and other spatial regions with large DM concentration did not show this signal.

- **Phase space** A lower bound on the mass of N_1 can be deduced from the phase space density in dwarf spheroidal galaxies accompanying the Milky Way. This is known as the Tremaine-Gunn bound. This gives the bound $M_{N_1} > 1$ keV.

- **DM production** We do not know exactly how and when DM was produced in the early universe. There are several possible ways for sterile neutrinos to be produced. These processes are beyond the scope of this thesis, but we can obtain constraints from them by demanding that they reproduce the correct DM relic density $\Omega_{DM} h^2$. An upper bound in the mass-mixing plane is derived from non-resonant thermal production. A lower bound can be found from resonant thermal production, which can occur if there is an asymmetry between leptons and anti-leptons during the production process.

Figure 6.2 shows the effect of the constraints on the allowed sterile neutrino DM mass and the total mixing contribution from the active neutrino states $\sum_\alpha \sin^2(2\theta_{\alpha 1})$. We

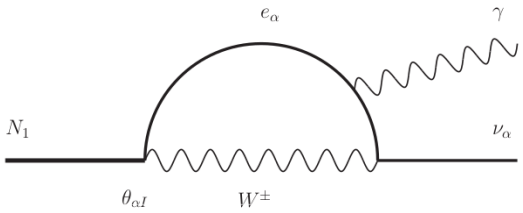

Figure 6.1: One possible radiative decay modes of the sterile neutrino $N_1 \to \gamma\nu_\alpha$. The coupling of N_1 to the W-boson is suppressed by the mixing angle $\theta_{\alpha i}$. [19]

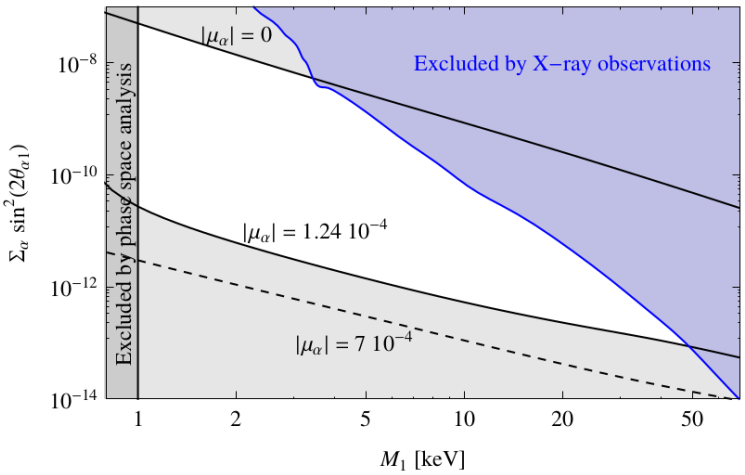

Figure 6.2: Constraints on sterile neutrino mass and mixing. The blue region is excluded by the X-ray observations. The region on the left with $M_{N_1} < 1$ eV is excluded by the Tremaine-Gunn bound. The black lines show the constraints derived from thermal production. The quantity μ_α is a measure for the lepton – anti-lepton asymmetry during production. Points on the lines recreate the correct DM relic density for the corresponding amount of lepton asymmetry. These bounds assume that all DM content consists of sterile neutrinos. [19]

construct a scatter plot of these same variables for our own model (using the mass eigenvalues of ν_4), the results of which can be seen in figure 6.3. We conclude that no points in our data set fall within the allowed DM region. Points that fall within the allowed mass range have mixing angles that are many orders too large, and points with allowed mixing angles are far too heavy. Possible explanations are our choice of parameter ranges for m_D and M_M and the scanning method. Since $\theta = m_D M_M^{-1}$, allowing larger values for M_M (while at the same time keeping one heavy neutrino light enough to fall within the DM mass bounds) could subdue the mixing angle for lower DM masses.

6.1 The νMSM

In this thesis we provide a solution for the lack of neutrino masses and DM in the minimal SM by adding three right-handed heavy neutrinos. There is a model known as the Neutrino Minimal SM that aims to do the same, and additionally explain the

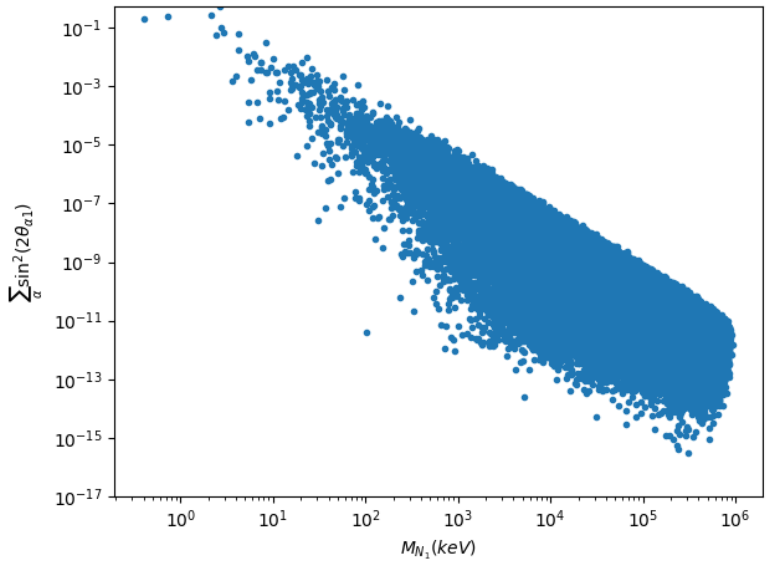

Figure 6.3: Scatter plot of the mass and the summed sterile-active mixing angle of the lightest sterile neutrino state ν_4.

asymmetry between the amount of baryonic matter and anti-matter in our universe [19]. The model is constructed to modify the SM as little as possible, and only adds three right-handed neutrino fields, just as we have done. It also relies on the type-I seesaw mechanism to provide light masses for the active neutrinos. In the pursuit of minimal new physics it does not introduce masses higher than the Z-boson mass for the sterile neutrinos. It has been shown that this model can simultaneously address these three problems in physics, but only under certain conditions. One sterile neutrino must have a mass in the keV range, and the other two must have equal masses within the range of 1 GeV up to $M_Z = 91$ GeV. This degeneracy in mass boosts the production of the lightest sterile neutrino through resonant effects, which is necessary to get the correct DM relic density [19]. Additionally the lightest sterile neutrino may not provide a significant contribution to the mass of the active neutrinos through the type-I seesaw mechanism, leaving one of them (nearly) massless.

If we compare these conditions to the mass eigenvalues we generated in figure 5.1 we can make a few observations. First, ν_6 has mass eigenvalues in the correct range for the νMSM, and there are values for ν_4 in the keV range. However, the mass eigenvalues for ν_5 generally fall below 1 GeV and have little overlap with ν_6 masses, so we are unlikely to have many points with degenerate masses that are high enough. Last, figure 5.1 seems to allow for nearly massless ν_1 neutrinos. The lightest ν_1 in our data set has a mass of the order $\mathcal{O}(10^{-15})$ eV, compared to a mean mass of 2.0×10^{-4} eV for all ν_1. In future research it would be interesting to see the effects of having degenerate masses for ν_5 and ν_6 in our model, and if it results in data points with correct mass splittings between the active neutrinos Δm^2_{ij} and with sterile neutrinos in the allowed DM region as shown in figure 6.2.

7. Conclusion

The goal of this thesis was to explore the possibilities of the type-I seesaw mechanism that expands on the SM, and accounts for both the small neutrino masses and a DM candidate. To accomplish this we introduced three new particles, the right-handed sterile neutrinos. These heavy particles generate masses for the left-handed neutrinos of the SM through the type-I seesaw mechanism and have the right properties that make them interesting DM candidates. To gain a better understanding of the behaviour of the type-I seesaw mechanism we performed a uniform parameter scan of the entries of the Majorana and Dirac mass matrices in the ranges $M_M \in [0 - 1 \cdot 10^9]$ eV and $m_D \in [0 - 1000]$ eV. We have a total of 12 free parameters in our model, and we have generated $\mathcal{O}(10^6)$ data points. In our data we reproduce the large mass difference between the sterile and active neutrinos that is emblematic of the type-I seesaw mechanism, and we see a clear distinction between the mass distributions of the three light and three heavy mass eigenstates. Our search did not produce a significant number of data points (exactly one) that reproduce the correct mass squared differences Δm^2_{ij} between the active neutrinos, which have been experimentally determined by observing neutrino oscillations. If we look at the ratio $\frac{\Delta m^2_{12}}{\Delta m^2_{23}}$ we find a total of 33150 points with values within the 3σ experimental uncertainty. We have plotted and analyzed the flavour mixing of the neutrino mass eigenstates. We see that especially ν_3, the heaviest of the light neutrino mass eigenstates, can have significant contributions from the sterile flavour eigenstates.

We have discussed the theoretical and experimental constraints that exist on sterile neutrinos as a DM candidate. These translate to bounds on the DM sterile neutrino mass and the active-sterile mixing angle θ that describes the strength of the mixing between the DM sterile neutrino and the active neutrino states (see figure 6.2). Again our search did not produce points in the non-excluded region, and points that fall in the correct keV mass range all mix too strongly with the active neutrinos.

Future research on this topic could focus on more targeted search efforts for points that have correct mass splittings between the active neutrinos and have a sterile neutrino that can act as DM. This could be achieved by varying the search ranges of the Dirac and Majorana mass matrix parameters and applying non-uniform distributions, or by specifically searching in the parameter space neighbourhood of data points close to the allowed regions. Inspiration can be taken from the νMSM. This model employs the type-I seesaw mechanism and, in addition to neutrino masses and DM, gives an explanation for the asymmetry between matter and anti-matter in the universe. Notably our model already produces masses for the sterile neutrinos in the correct ranges for the νMSM, but it does not comply to the demand that

there are two GeV-range sterile neutrinos with approximately degenerate mass and one keV sterile neutrino that mixes very weakly with the active neutrinos. A next step could be enforcing these νMSM constraints on our model and comparing the resulting data set to the data used for this thesis.

Bibliography

[1] A. Boyarsky, M. Drewes, T. Lasserre, S. Mertens, and O. Ruchayskiy. Sterile neutrino dark matter. *Progress in Particle and Nuclear Physics*, 104:1–45, 2019.

[2] N. Aghanim and et al. Planck 2018 results. *Astronomy & Astrophysics*, 641:A6, 2020.

[3] K Freese. Status of dark matter in the universe. *International Journal of Modern Physics D*, 26(06):1730012, 2017.

[4] M. Bauer and T Plehn. *Yet Another Introduction to Dark Matter*. Lecture Notes in Physics. Springer, 2018.

[5] P. A. R. Ade and et al. Planck2013 results. i. overview of products and scientific results. *Astronomy & Astrophysics*, 571:A1, 2014.

[6] K. Abazajian and et al. Light sterile neutrinos: A white paper. *arXiv: 1204.5379*, 2012.

[7] F. Maltoni, J. M. Niczyporuk, and S. Willenbrock. Upper bound on the scale of majorana-neutrino mass generation. *Physical Review Letters*, 86(2):212–215, Jan 2001.

[8] D. J. Griffiths. *Introduction to elementary particles; 2nd rev. version*. Physics textbook. Wiley, New York, NY, 2008.

[9] S. Bilenky. *Introduction to the physics of massive and mixed neutrinos*, volume 817. 2010.

[10] M. E. Peskin and D. V. Schroeder. *An introduction to quantum field theory*. Westview, Boulder, CO, 1995.

[11] P. Lipari. Introduction to neutrino physics. In *1st CERN-CLAF School of High-Energy Physics*, pages 115–199, 2001.

[12] B Meszéna. Neutrino oscillations. *Wolfram Demonstrations Project*.

[13] I. Esteban and et al. The fate of hints: updated global analysis of three-flavor neutrino oscillations. *Journal of High Energy Physics*, 2020(9), 2020.

[14] S. Vagnozzi. Weigh them all! - cosmological searches for the neutrino mass scale and mass ordering. *Springer Theses*, 2019.

[15] W. Flieger and J. Gluza. General neutrino mass spectrum and mixing properties in seesaw mechanisms. *Chin. Phys. C*, 45(2):023106, 2021.

[16] Philip D. Powell. Calculating determinants of block matrices. *arXiv: 1112.4379*, 2011.

[17] M. Drewes and et al. A White Paper on keV Sterile Neutrino Dark Matter. *JCAP*, 01:025, 2017.

[18] B. Roskovec. Neutrino physics with reactors, 2018.

[19] M. Drewes. The phenomenology of right handed neutrinos. *International Journal of Modern Physics E*, 22(08):1330019, 2013.

A. Mass Eigenstate Decompositions

This appendix contains the scatter plots of the flavour composition of all six mass eigenstates, as explained in chapter 5.3. We use the following notation for $U^*\nu_\alpha = \nu_i$:

$$\begin{pmatrix} U_{00} & U_{10} & U_{20} & U_{30} & U_{40} & U_{50} \\ U_{01} & U_{11} & U_{21} & U_{31} & U_{41} & U_{51} \\ U_{02} & U_{12} & U_{22} & U_{32} & U_{42} & U_{52} \\ U_{03} & U_{13} & U_{23} & U_{33} & U_{43} & U_{53} \\ U_{04} & U_{14} & U_{24} & U_{34} & U_{44} & U_{54} \\ U_{05} & U_{15} & U_{25} & U_{35} & U_{45} & U_{55} \end{pmatrix} \cdot \begin{pmatrix} \nu_e \\ \nu_\mu \\ \nu_\tau \\ \nu_{s_1} \\ \nu_{s_2} \\ \nu_{s_3} \end{pmatrix} = \begin{pmatrix} \nu_6 \\ \nu_5 \\ \nu_4 \\ \nu_3 \\ \nu_2 \\ \nu_1 \end{pmatrix}$$

The colours indicate which flavour eigenstate provides the greatest contribution to the total mixing of the mass eigenstate for each data point.

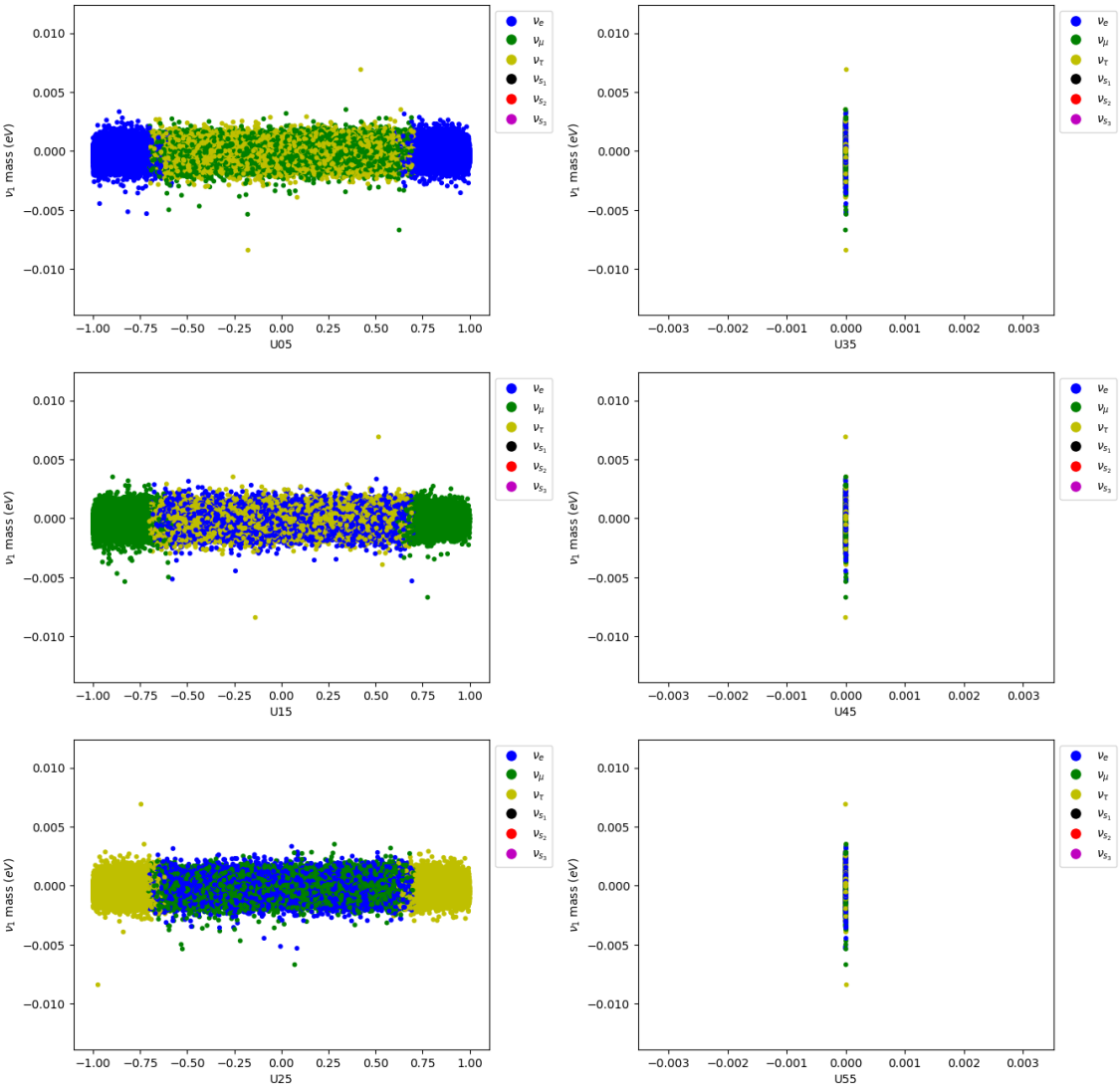

Figure A.1: ν_1 flavour composition

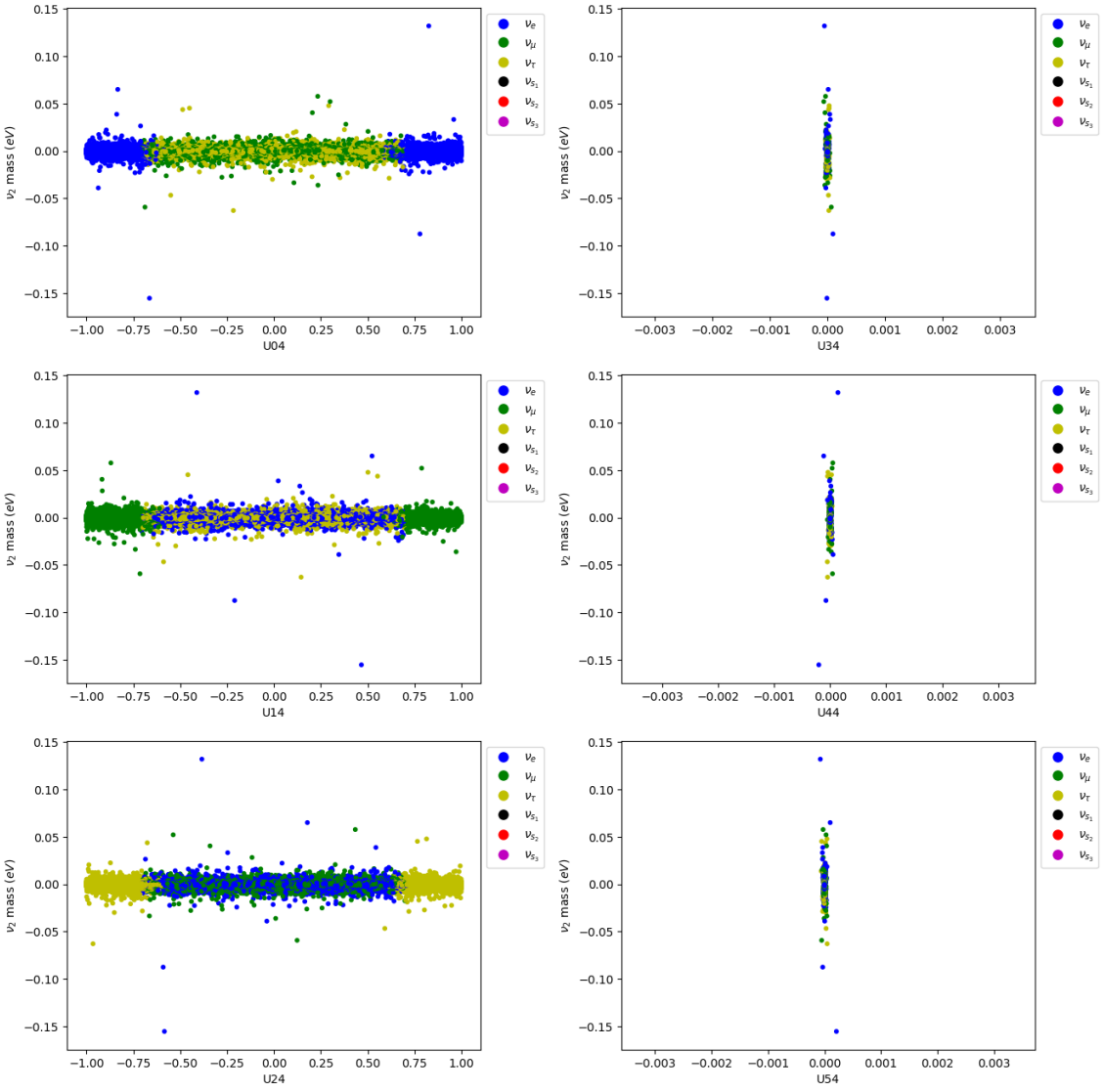

Figure A.2: ν_2 flavour composition

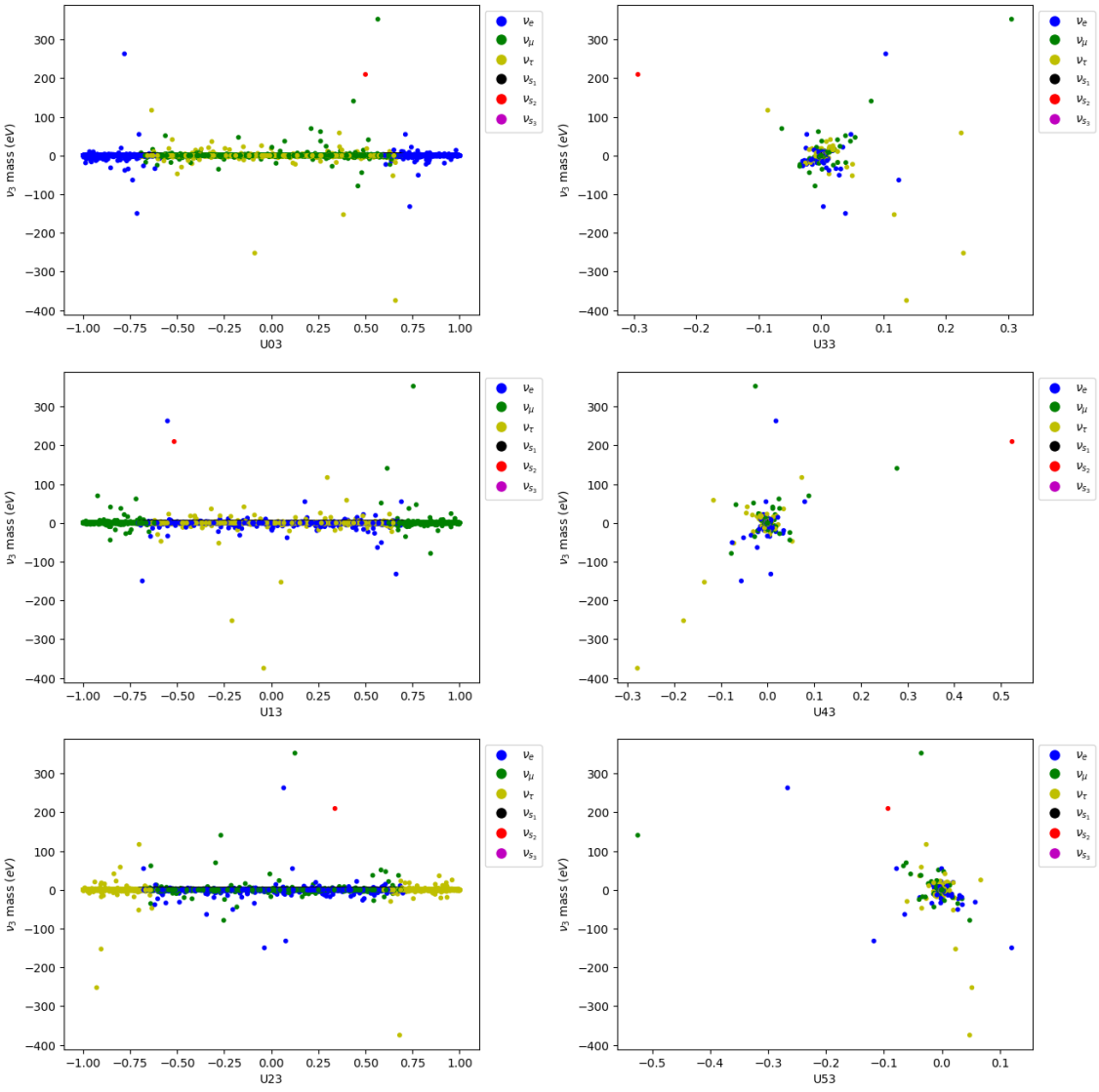

Figure A.3: ν_3 flavour composition

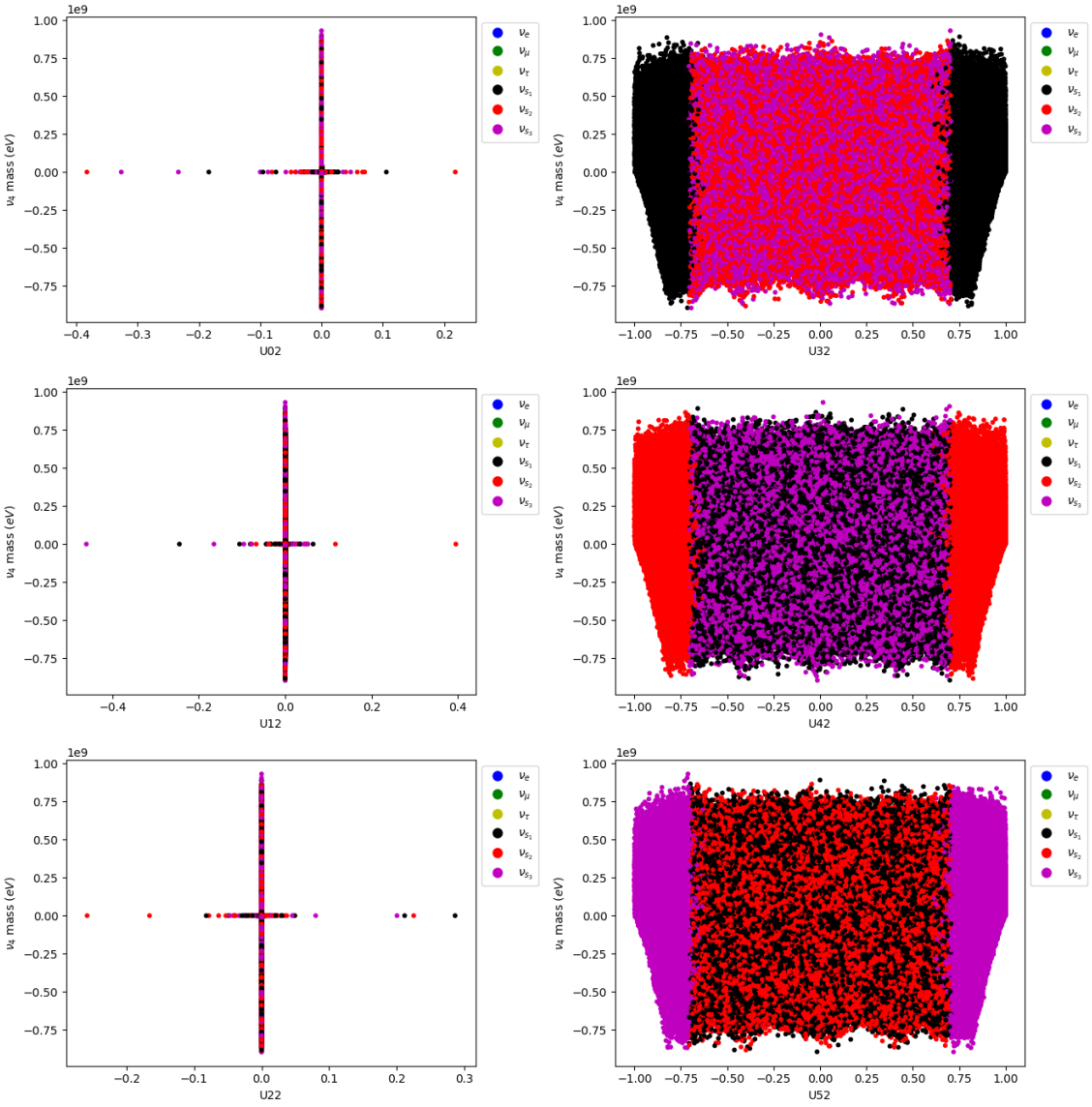

Figure A.4: ν_4 flavour composition

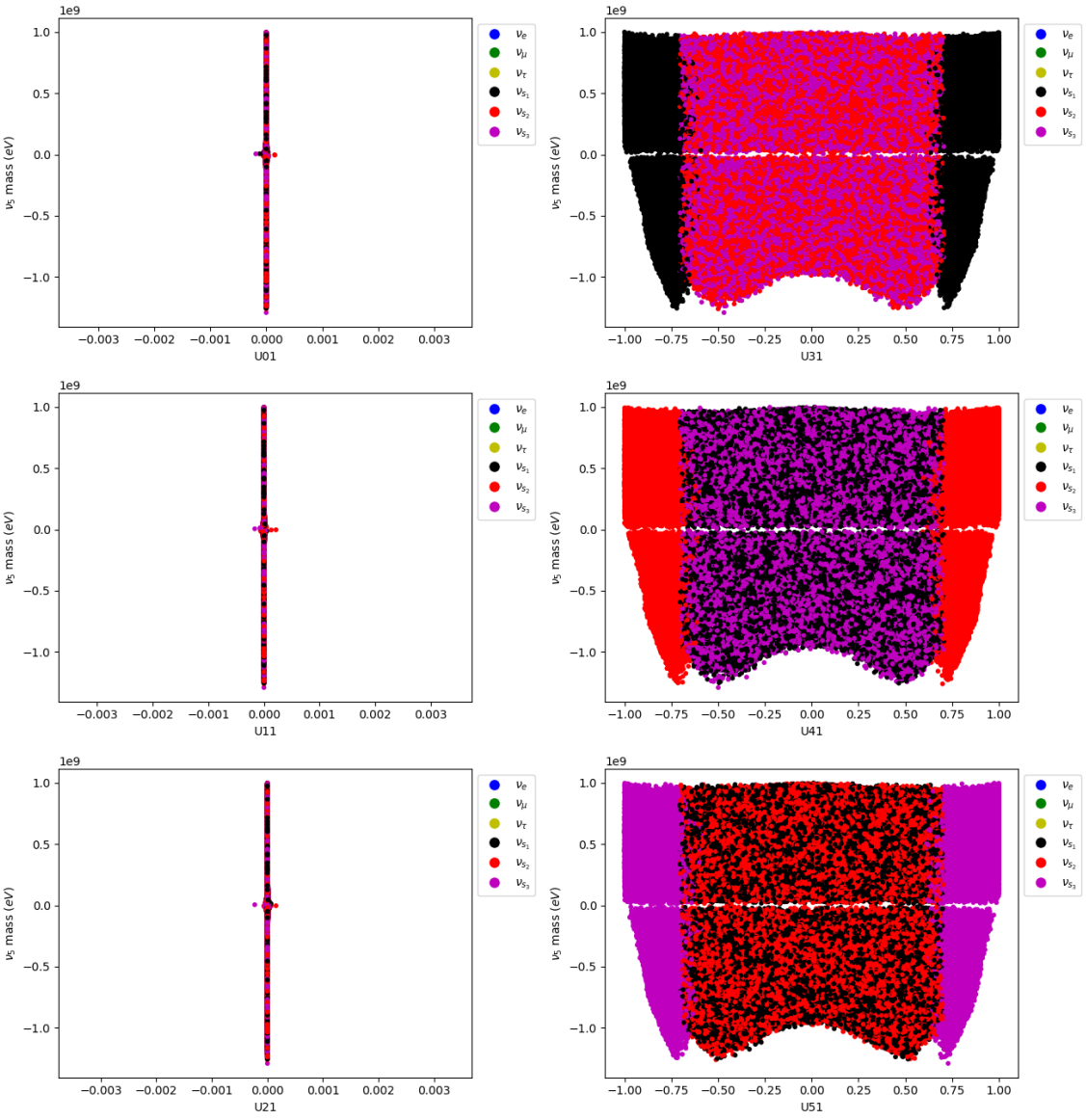

Figure A.5: ν_5 flavour composition

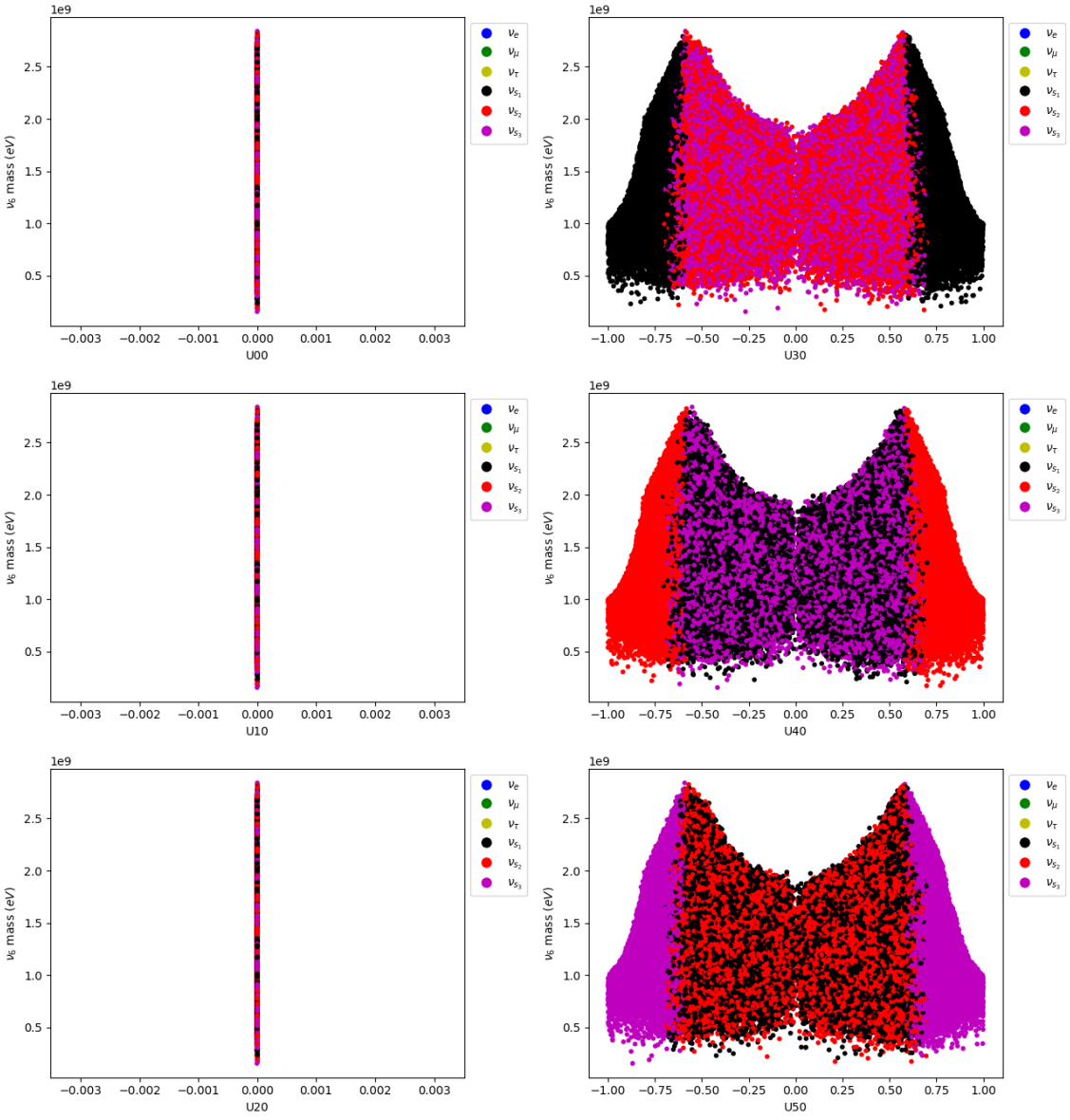

Figure A.6: ν_6 flavour composition